

# Rapid and even spreading of complex fluids over a large area in porous substrates

Prashant Agrawal,<sup>1</sup> Hemant Kumar,<sup>2</sup> and Praseon Kumar<sup>2, 3, a)</sup>

<sup>1)</sup>*Smart Materials and Surfaces Laboratory, Faculty of Engineering and Environment, Northumbria University, Newcastle upon Tyne, NE1 8ST, United Kingdom*

<sup>2)</sup>*Biomaterials and Tissue Engineering Lab, Materials Engineering, Indian Institute of Science, Karnataka, 560054, India*

<sup>3)</sup>*Department of Biotechnology and Medical Engineering, National Institute of Technology, Rourkela, Odisha, 769001, India*

(Dated: 23 July 2020)

Rapid and even spreading of complex fluids over a large area on substrates like paper is required for chemical and biological sensing applications. Non-Newtonian flow behaviour and presence of multi-phase components poses a significant challenge to uniform flow in porous media. Specially in case of blood, for bio-sensing applications, fast spread on a large area is required to avoid coagulation and non-uniform component spread. In this work we have developed a filter paper based device to resolve this spreading challenge. We sandwich the filter paper between a matrix of nanofibrous membrane backed by polyethylene terephthalate (PET) sheets, forming a multi-scale pore network: one within the filter paper and the other between the PET sheet and the filter paper. By doing so, we decrease the overall resistance to flow while maintaining the same capillary suction pressure to obtain a quick, uniform spread of dyed liquids, milk solutions and whole blood. The device design and concepts used here can be used in paper microfluidic applications and to develop devices for Dried Blood Spot analysis that utilize this fast flow while maintaining even spreading over a large area.

Lab-on-chip devices have emerged as useful tools for applications in rapid and efficient analytical chemistry, sensing and diagnostics, and bioengineering<sup>1-3</sup>. These devices primarily depend on a power source to drive small volumes of liquid samples in specially designed micro/nanochannels to achieve their objectives. Here, paper microfluidics has emerged as a viable alternative to create lab-on-chip devices, which can drive liquids passively using capillary suction<sup>4</sup>. The advantages offered by paper based devices is that they are simple to operate, amenable to scale-up manufacturing, easily deployable in resource constraint places and cost-effective<sup>5</sup>. To develop devices for applications in point-of-care diagnostics<sup>6</sup> it is important to develop devices which can passively drive complex fluids, like blood and saliva. Here, fluid properties like non-Newtonian flow behavior and interaction of active and passive bio-matter with the interconnected pores of a paper presents significant variability in flow behavior.

Several works have addressed fluid flow enhancements in porous substrates<sup>7</sup>, primarily for Newtonian fluids, by either altering the base porous material properties<sup>8,9</sup> or novel device design<sup>10,11</sup>. These methods primarily alter the fundamental passive transport properties, such as, increasing capillary suction pressure or reducing resistance to fluid flow. Strategies such as the use of alternate materials (e.g. fibrous paper<sup>8</sup>, hydrogels<sup>12</sup>, cellulose<sup>13</sup>), pore interconnectivity<sup>14</sup>, designed pore gradients<sup>15,16</sup>, evaporation assisted pumping<sup>17,18</sup>, integration of hydrophilic backing materials<sup>19</sup> and layered substrate designs<sup>20,21</sup> have shown significant success in transporting Newtonian fluids, with a potential of extrapolation to complex fluids. However, very few designs address flow nature of complex fluids like blood<sup>22-24</sup>, semen<sup>25</sup> and saliva<sup>26</sup>,

which have significant implications in bio-analysis for diagnostic and pharmaceutical applications.

In this work, we present a device that enhances the capillary suction of complex colloidal liquids in a normal filter paper. We utilize a multi-scale porous network design that retains the capillary suction of the filter paper, while easing the flow of fluid through an integrated relatively larger pore network. We show that this device enhances the imbibition for both Newtonian and non-Newtonian liquids by using dyed water, skimmed milk solution in water and whole blood. The device not only allowed enhanced flows rate but also enabled even spreading of the colloidal liquids. We explain these observations using an analytical model employing Darcy's law and a hydraulic circuit analogy. The proposed concept and designs have implications in increasing sensitivity and reliability of paper based sensors and diagnostic devices.

A polymer solution of Polycaprolactone (PCL) and porcine skin gelatin was prepared for electrospinning. First, two separate solutions of PCL and gelatin in 2, 2, 2 trifluoro ethanol solvent were prepared (12 % wt/vol). Both the solutions were kept for overnight stirring at room temperature (IKA C-MAGHS7 digital). After the overnight stirring, both solutions were mixed followed by an addition of 50  $\mu$ l of pure glacial acetic acid to generate a clear, transparent PCL/gelatin solution. The polymer solutions were fed into 5 ml clinical syringe and electrospinning was carried using a computer-controlled electrospinning apparatus (ESPIN NANO, Physics Instruments Co.) with the following parameters: flow rate of 0.5 ml h<sup>-1</sup>, voltage of 10 kV, needle gauge 24 and distance between electrodes 150 mm. The nanofibers were deposited on thin cellulose acetate (PET) sheet which were then laid over a thin strip of Whatman filter paper (width 10 mm and height 60 mm). This method was followed to prepare the one sided and two sided samples. The dye solution of methylene blue

<sup>a)</sup>Electronic mail: praseonkumar1985@gmail.com

dye (M-dye) and orange food dye (O-dye) in water (1 percent wt/vol) was prepared to study thin layer chromatography (TLC) effect in filter paper. The simulated blood sample was prepared by adding milk (skim milk powder) and de-ionized water to form solutions of different density (0 -50 % wt/vol) to study the capillary rise through filter paper. The solutions with different milk concentrations were sonicated for 10 minutes to obtain a homogenous solution<sup>27</sup>. Gift blood samples were received from a pathology lab owned by Molecular Solution care Health LLP, Bengaluru

For the spreading studies, the devices were held vertically with the help of a clamp stand. The liquid reservoir was placed on a lab-jack for manual vertical movement. The reservoir is slowly raised to contact the device. After 60 seconds from the time of first contact, the reservoir is promptly lowered and the height achieved by liquid in the filter paper is noted. This experiment is repeated multiple times for each of the liquids (O-dyed and M-dyed water, milk solutions and whole blood) for each of the three device designs: native filter paper, filter paper supported on one side by electrospun nanofiber sheet (one-side) and filter paper sandwiched between electrospun nanofiber sheet (two-side).

Figure 1 shows the imbibed length of dyed water in the different substrate designs after 1 minute. The sandwich designs are clearly seen to drive a higher volume of liquid compared to the bare filter paper substrate. The dyed solutions undergo a chromatographic separation, wherein, the water wetting front advances further leaving a separate dye front. The methylene blue dye has a higher molecular weight and, therefore, imbibes a shorter distance compared to the orange dye. As a result, the difference in the imbibed height of the wetting front and the dyed front is less significant for the orange dye compared to the methylene blue dye, as seen in Figure 1.

The enhancement in flow in the sandwiched designs compared to the native filter paper designs can be qualitatively explained by observing the porous network structure in the design (Figure 3). The small pores in the filter paper generate a high capillary pressure, while also restricting the flow, which leads to a slow moving wetting front. By placing a nanofibrous membrane (with larger pore sizes than the filter paper), the sandwich designs retain the high suction pressure of the filter paper and provide an easier pathway to the flow within the fibrous membrane structure, supported by a hydrophilic backing material. Subsequently, through this multi-scale porous network we obtain a much faster spread in the sandwich designs as compared to the native filter paper.

To quantify the difference in imbibition characteristics of the three designs, we use Darcy's law for characterizing the flow in the porous media<sup>28</sup>:

$$v = \frac{k}{\mu\phi} \nabla p, \quad (1)$$

where,  $v$  is the velocity of the wetting front,  $k$  is the permeability of the liquid in the substrate,  $\mu$  is the dynamic viscosity of the liquid,  $\phi$  is the porosity of the substrate and  $\nabla p$  is the pressure difference driving the flow. In our vertical imbibition setup (against gravity), the flow is driven by the capillary pressure in the pores of the filter paper ( $p_c$ ). As a result equation

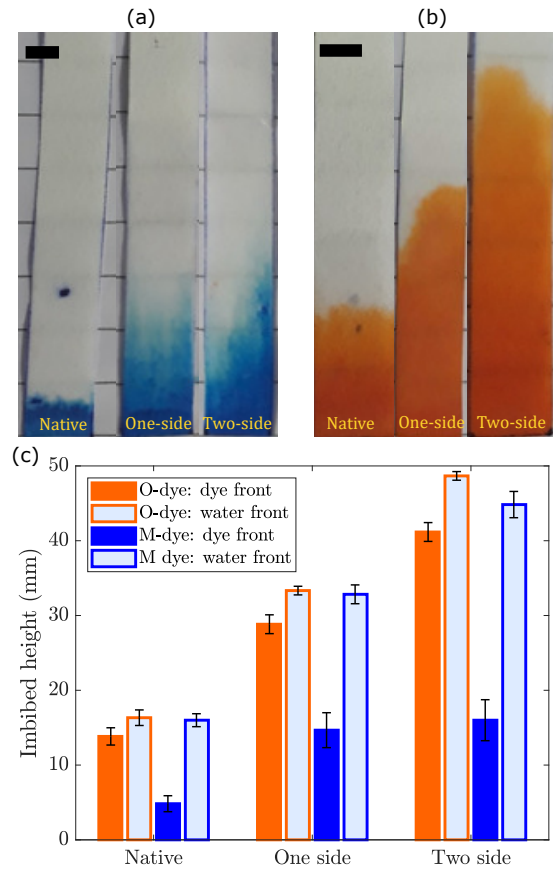


FIG. 1: Vertical imbibition results with dyed water: (a) Methylene blue dye (M-dye) in de-ionized water, (b) Orange dye (O-dye) in de-ionized water; scale bar is equivalent to 5 mm (c) Position of the wetting front recorded after 60 seconds from the start of imbibition for the native filter paper, one-sided and two-sided sandwiched filter paper design. The plot shows the dye front and the water wetting front due to chromatographic separation of the dye.

1 can be written as:

$$\frac{dh}{dt} = \frac{k}{\mu\phi} \frac{(p_c - \rho_l g h)}{h}, \quad (2)$$

where,  $h$  is the height of the wetting front,  $\rho_l$  is the density of the liquid,  $g$  is the acceleration due to gravity,  $p_c = \rho_w g h_c$ ,  $\rho_w$  is the density of water and  $h_c$  is the capillary pressure head<sup>18</sup>. Assuming the density difference to be comparable, i.e.  $\rho_l \approx \rho_w$ , the solution to equation 2 is obtained as:

$$\frac{h}{h_c} + \log \left( 1 - \frac{h}{h_c} \right) = - \frac{kg\rho_l}{\phi h_c \mu} t \quad (3)$$

By using equation 3 we can obtain the value of permeability  $k$  for the three substrate designs. For an appropriate design comparison across different complex liquids it is important to isolate the value of  $k$  from the other parameters. However, isolating this value of  $k$  accurately is extremely challenging, as

evaluating the other parameters requires measuring additional material properties ( $\phi$ ,  $h_c$ ) and liquid properties ( $\rho_l$ ,  $\mu$ ) accurately through different experiments which are highly sensitive in their setup and measurement<sup>29,30</sup>. We also avoid the use of equivalent models, like the Kozeny-Carman capillary model<sup>31,32</sup> to calculate and compare the permeability for these designs as such models are approximations and require information about the porous medium's microscopic properties like pore geometry and tortuosity, which are difficult to measure accurately<sup>33,34</sup>. Instead, we use equation 3 with our experimental data to calculate the parameter  $K_i = k_i g \rho_l / (\phi_i h_c \mu)$ , where  $i = 0, 1$  and  $2$  for the native filter paper, single side and double sided substrate, respectively. For a given liquid, this apparent permeability ( $K_i$ ) is an indirect method of comparing the ease of flow of liquid through the different substrates, calculated from equation 4.

$$\frac{h}{h_c} + \log \left( 1 - \frac{h}{h_c} \right) = -Kt \quad (4)$$

TABLE I: Apparent permeability ( $K_i$ ) of the native filter paper ( $K_0$ ), one-sided ( $K_1$ ) and two-sided ( $K_2$ ) sandwich designs obtained from equation 4.

Liquid		$K_0 (\times 10^6)$	$K_1 (\times 10^6)$	$K_2 (\times 10^6)$
O-dye	Dye front	$1.61 \pm 0.07$	$7.07 \pm 0.62$	$14.53 \pm 0.90$
	Liquid front	$2.25 \pm 0.29$	$9.47 \pm 0.33$	$20.40 \pm 0.49$
M-dye	Dye front	$0.19 \pm 0.01$	$1.84 \pm 0.59$	$2.2 \pm 0.77$
	Liquid front	$2.16 \pm 0.23$	$9.19 \pm 0.71$	$17.28 \pm 1.37$

In Table I we calculate the apparent permeability ( $K_i$ ) for the three substrates for the liquid and dye wetting front for the two dyes shown in Figure 1 and clearly observe higher values for the sandwich designs. We can understand the increase in apparent permeability for the sandwich designs using the principle of equivalent hydraulic resistance. As shown in Figure 2, the sandwich designs can be considered as two different porous media arranged in parallel, where the permeability of flow in the native filter paper is  $k_0 = k_{fp}$  and that in the nanofibrous channel is  $k_{np}$ .  $k_{np}$  is obtained from the equivalent permeability of the one-sided design ( $k_1 = k_{fp} + k_{np}$ ), which can then be used to predict the permeability of the two-sided design by  $k_2 = k_{fp} + 2k_{np}$ . This equivalence can also be extended to the parameter  $K_i$  when using data for the same imbibing liquids. As seen from the data in Table I, this simplistic equivalent resistance argument (i.e.,  $K_2 \approx K_0 + 2K_1$ ) agrees well with the experimental values for all the wetting fronts except the methylene blue dye front (due to early chromatographic separation).

This enhancement in permeability to flow by our sandwich designs is not only limited to Newtonian liquids but also to complex liquids exhibiting a non-Newtonian flow behavior, as shown in Figure 3 and Figure 4 for milk and blood, respectively. Blood is a complex fluid with multiple particulate and active bio-matter, while milk has been shown to demonstrate complex non-Newtonian flow behavior at different concentrations in water<sup>27,35,36</sup>. Estimating the flow characteristics of

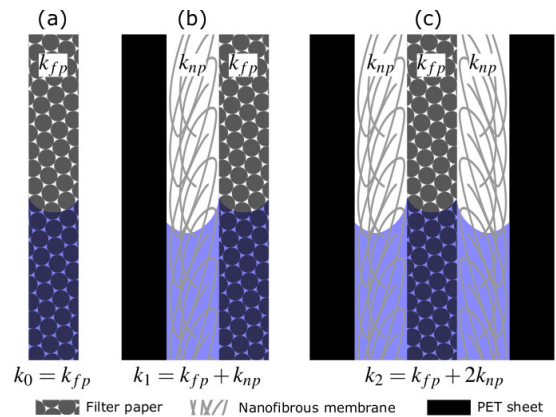


FIG. 2: Depiction of the devices used in our experiments and their associated permeability relations: (a) native filter paper, (b) one-sided sandwich design and (c) two-sided sandwich design.

these liquids becomes challenging in porous media as imbibition speed, presence of particulate matter and protein interaction affect their viscosity and, by extension, resistance to flow. Especially in blood sampling applications, like Dried Blood Spot analysis, the general variability in hematocrit volume (volume percentage of red blood cells) of blood amongst individuals poses challenge during formation of consistent size and uniformity of blood spots. This leads to poor adoption of the dried blood spot technique for any quantitative analysis in pharmaceutical and diagnostic field<sup>37</sup>. Hence, a qualitative blood flow characterization provides sufficient utility than an accurate quantitative flow characterization for diagnostic applications as such accuracy is very difficult to achieve. Therefore, in order to compare the enhancement in ease of flow of complex fluids in our designs, we retain the above presented simplistic Newtonian approach.

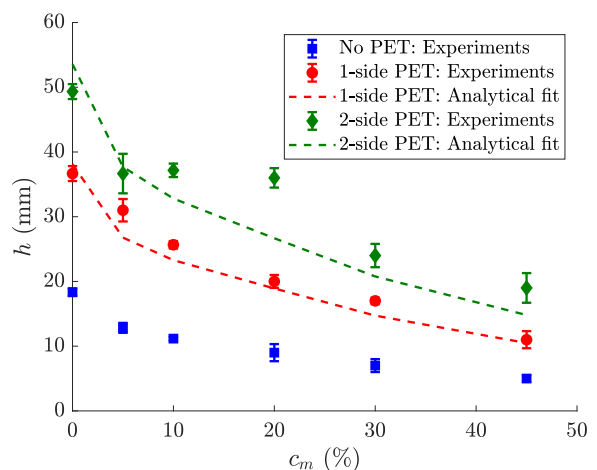


FIG. 3: Imbibed height  $h$  for different concentrations of milk powder in water ( $c_m$ ) for different substrate types: native filter paper, one-side sandwiched paper and two-sided sandwiched paper.

To demonstrate the enhanced permeability of the sandwich designs for each of the liquids with different milk concentration, we obtain the apparent permeability for the filter paper design, i.e.,  $K_0$ , from their imbibed height after 1 minute. Then, using the factors obtained from Table I ( $K_1 \approx 4.3K_0$  and  $K_2 \approx 2K_0$ ), we obtain  $K_1$  and  $K_2$  for each of the liquids (with different milk concentrations) and analytically calculate the imbibed height after 1 minute using equation 3, and compare it with the experimental data in Figure 3. As seen in Figure 3, the permeability enhancements obtained for dyed water also agree with a wide range of milk solutions, spanning Newtonian and non-Newtonian fluid flow behavior. Similar agreement is obtained for the devices with blood flow (Figure 4), where  $K_0 = 0.20 \pm 0.11 \times 10^{-6}$ ,  $K_1 = 1.90 \pm 0.55 \times 10^{-6}$  and  $K_2 = 3.88 \pm 0.93 \times 10^{-6}$ .

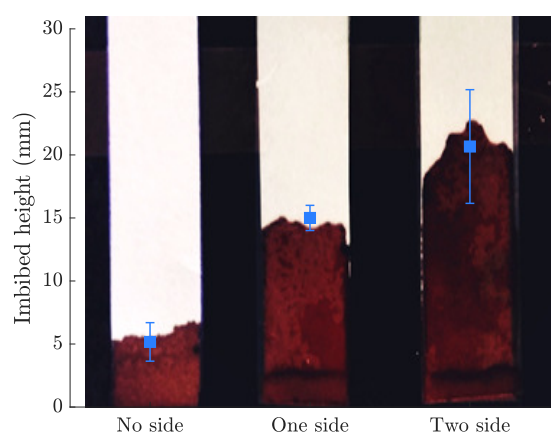


FIG. 4: Comparison of vertical imbibition of blood in the three paper designs.

Our presented sandwich device design utilizes a multi-scale porous network to provide an enhanced capillary suction pressure (because of smaller pores) and a low resistance to liquid flow (due to the larger porous matrix). The speed and uniformity of liquid suction in a porous substrate depends on the nature of the liquid. We have shown our sandwich designs pump both Newtonian and non-Newtonian liquids uniformly at high speeds without significant chromatographic effects. Our initial results on pumping and spreading complex colloidal fluids, like milk and blood, in a filter paper are promising to develop paper-based diagnostic sensor using whole blood sample. The potential future of this work lies in integrating this multi-scale porous network design concept in devices for dried blood spots and biosensors. Integration with sensor electronics present additional questions on the effect of charges on flow and particle behavior. For example, the presence of charges on the paper will increase the hydrophilicity for an enhanced capillary pumping and also provide platforms for bio-conjugation of antibodies for sensing applications<sup>38</sup>. The microporous filter paper can also be coated with nanofibrous polymers that can provide additional surface with desired charges for bio-conjugation<sup>39</sup>.

## ACKNOWLEDGMENTS

Authors would acknowledge the Prof. Kaushik Chatterjee, IISc Bangalore for providing lab infrastructure and resources for conducting the experimental work. Authors also thank Molecular Solution Care health LLP, Bengaluru for providing the patients blood samples. PK would like to acknowledge BIG BIRAC grant BIRAC/IKP0664/BIG-12/18, DBT, Govt. of India for funding the project. HK acknowledges Indian Academy of Sciences for summer internship fellowship at IISc Bangalore

## DATA AVAILABILITY STATEMENT

The data that support the findings of this study are available from the corresponding author upon reasonable request.

## REFERENCES

- K. Yamada, H. Shibata, K. Suzukia, and D. Citterio, "Toward practical application of paper-based microfluidics for medical diagnostics: state-of-the-art and challenges," *Lab on a chip* **17**, 1206–1249 (2017).
- D. Figeys and D. Pinto, "Lab-on-a-chip: A revolution in biological and medical sciences," *Analytical Chemistry* **72**, 330A – 335A (2000).
- E. K. Sackmann, A. L. Fulton, and D. J. Beebe, "The present and future role of microfluidics in biomedical research," *Nature* **507**, 181–189 (2014).
- H. Lim, A. T. Jafry, and J. Lee, "Fabrication, flow control, and applications of microfluidic paper-based analytical devices," *Molecules* **24**, 2869 (2019).
- X. Li, D. R. Ballerini, and W. Shen, "A perspective on paper-based microfluidics: Current status and future trends," *Biomicrofluidics* **6**, 11301–1130113 (2012).
- M. Sher, R. Zhuang, U. Demirci, and W. Asghar, "Paper-based analytical devices for clinical diagnosis: recent advances in the fabrication techniques and sensing mechanisms," *Expert review of molecular diagnostics* **17**, 351–366 (2017).
- S. Kumar, P. Bhushan, and S. Bhattacharya, *Fluid Transport Mechanisms in Paper-Based Microfluidic Devices*, Advanced Functional Materials and Sensors (Springer, Singapore, 2019) pp. 7–28.
- F. Carstens, J. A. Gamelas, and S. Schabel, "Engineering microfluidic papers: determination of fibre source and paper sheet properties and their influence on capillary-driven fluid flow," *Cellulose* **24**, 295–309 (2017).
- Q. B. Meng, Z. Z. Gu, O. Sato, and A. Fujishima, "Fabrication of highly ordered porous structures," *Applied Physics Letters* **77**, 4313–4315 (2000).
- W. C. Lee, Y. J. Heo, and S. Takeuchi, "Wall-less liquid pathways formed with three-dimensional microring arrays," *Applied Physics Letters* **101** (2012), 10.1063/1.4752720.
- W. Guo, J. Hansson, and W. Van Der Wijngaart, "Capillary Pumping Independent of Liquid Sample Viscosity," *Langmuir* **32**, 12650–12655 (2016).
- T. D. Wheeler and A. D. Stroock, "The transpiration of water at negative pressures in a synthetic tree," *Nature* **455**, 208–212 (2008).
- J. Kim, J. Ha, and H. Y. Kim, "Capillary rise of non-aqueous liquids in cellulose sponges," *Journal of Fluid Mechanics* **818**, 1–12 (2017).
- A. Olanrewaju, M. Beaugrand, M. Yafia, and D. Juncker, "Capillary microfluidics in microchannels: from microfluidic networks to capillary circuits," *Lab Chip* **18**, 2323–2347 (2018).
- S. Ashraf and J. Phirani, "Capillary displacement of viscous liquids in a multi-layered porous medium," *Soft Matter* **15**, 2057–2070 (2019).
- C. H. Choi, S. Krishnan, W. TeGrotenhuis, and C. H. Chang, "Capillary rise of nanostructured microwicks," *Micromachines* **9**, 1–14 (2018).
- J. M. Li, C. Liu, K. P. Zhang, X. Ke, Z. Xu, C. Y. Li, and L. D. Wang, "A micropump based on water potential difference in plants," *Microfluidics and Nanofluidics* **11**, 717–724 (2011).

- <sup>18</sup>P. Agrawal, P. S. Gandhi, M. Majumder, and P. Kumar, "Insight into the Design and Fabrication of a Leaf-Mimicking Micropump," *Physical Review Applied* **12**, 1 (2019).
- <sup>19</sup>S. Mukhopadhyay, J. P. Banerjee, and S. S. Roy, "Effects of liquid viscosity, surface wettability and channel geometry on capillary flow in SU8 based microfluidic devices," *International Journal of Adhesion and Adhesives* **42**, 30–35 (2013).
- <sup>20</sup>C. K. Camplisson, K. M. Schilling, W. L. Pedrotti, H. A. Stone, and A. W. Martinez, "Two-ply channels for faster wicking in paper-based microfluidic devices," *Lab on a Chip* **15**, 4461–4466 (2015).
- <sup>21</sup>D. Shou and J. Fan, "Design of Nanofibrous and Microfibrous Channels for Fast Capillary Flow," *Langmuir* **34**, 1235–1241 (2018).
- <sup>22</sup>W. Guo, J. Hansson, and W. van der Wijngaart, "Capillary pumping independent of the liquid surface energy and viscosity," *Microsystems and Nanoengineering* **4** (2018), 10.1038/s41378-018-0002-9.
- <sup>23</sup>S. D. Polley, D. Bell, J. Oliver, F. Tully, M. D. Perkins, P. L. Chiodini, and I. J. González, "The design and evaluation of a shaped filter collection device to sample and store defined volume dried blood spots from finger pricks," *Malaria Journal* **14**, 1–7 (2015).
- <sup>24</sup>R. Sturm, J. Henion, R. Abbott, and P. Wang, "Novel membrane devices and their potential utility in blood sample collection prior to analysis of dried plasma spots," *Bioanalysis* **7**, 1987–2002 (2015).
- <sup>25</sup>M. Koji, K. Chen, C. Tsai, L. Wenqian, A. Yuka, N. Keiji, and C. Cheng, *Microfluidics and Nanofluidics* **16**, 857–867 (2014).
- <sup>26</sup>L. de Castro, S. de Freitas, L. C. Duarte, J. de Souza, T. Paixão, and W. Coltro, "Salivary diagnostics on paper microfluidic devices and their use as wearable sensors for glucose monitoring," *Analytical and Bioanalytical Chemistry* **4**, 4919–4928 (2019).
- <sup>27</sup>T. Panchal, N. Spooner, and M. Barfield, "Ensuring the collection of high-quality dried blood spot samples across multisite clinical studies," *Bioanalysis* **9**, 209–213 (2017).
- <sup>28</sup>D. Ingham and I. Pop, *Transport Phenomena in Porous Media* (Pergamon Press, Danvers, MA, 1998).
- <sup>29</sup>R. Arbter, J. M. Beraud, C. Binetruy, L. Bizet, J. Bréard, S. Comas-Cardona, C. Demaria, A. Endruweit, P. Ermanni, F. Gommer, S. Hasanovic, P. Henrat, F. Klunker, B. Laine, S. Lavanchy, S. V. Lomov, A. Long, V. Michaud, G. Morren, E. Ruiz, H. Sol, F. Trochu, B. Verleye, M. Wietgreffe, W. Wu, and G. Ziegmann, "Experimental determination of the permeability of textiles: A benchmark exercise," *Composites Part A: Applied Science and Manufacturing* **42**, 1157–1168 (2011).
- <sup>30</sup>N. Vernet, E. Ruiz, S. Advani, J. B. Alms, M. Aubert, M. Barbarski, B. Barari, J. M. Beraud, D. C. Berg, N. Correia, M. Danzi, T. Delavrière, M. Dickert, C. Di Fratta, A. Endruweit, P. Ermanni, G. Francucci, J. A. Garcia, A. George, C. Hahn, F. Klunker, S. V. Lomov, A. Long, B. Louis, J. Maldonado, R. Meier, V. Michaud, H. Perrin, K. Pillai, E. Rodriguez, F. Trochu, S. Verheyden, M. Wietgreffe, W. Xiong, S. Zaremba, and G. Ziegmann, "Experimental determination of the permeability of engineering textiles: Benchmark II," *Composites Part A: Applied Science and Manufacturing* **61**, 172–184 (2014).
- <sup>31</sup>S. Sharma and D. A. Siginer, "Permeability Measurement Methods in Porous Media of Fiber Reinforced Composites," *Applied Mechanics Reviews* **63**, 020802 (2010).
- <sup>32</sup>J. Bear, *Dynamics of Fluids in Porous Media* (Dover Publications, New York, 2013).
- <sup>33</sup>K. M. Pillai, "Modeling the unsaturated flow in liquid composite molding processes: A review and some thoughts," *Journal of Composite Materials* **38**, 2097–2118 (2004).
- <sup>34</sup>M. Alava, M. Dubé, and M. Rost, "Imbibition in disordered media," *Advances in Physics* **53**, 83–175 (2004).
- <sup>35</sup>K. R. Morison, J. P. Phelan, and C. G. Bloore, "Viscosity and non-newtonian behaviour of concentrated milk and cream," *International Journal of Food Properties* **16**, 882–894 (2013).
- <sup>36</sup>M. Brust, C. Schaefer, R. Doerr, L. Pan, M. Garcia, P. E. Arratia, and C. Wagner, "Rheology of human blood plasma: Viscoelastic versus Newtonian behavior," *Physical Review Letters* **110**, 6–10 (2013).
- <sup>37</sup>P. Kumar, P. Agrawal, and K. Chatterjee, "Challenges and opportunities in blood flow through porous substrate: A design and interface perspective of dried blood spot," *Journal of Pharmaceutical and Biomedical Analysis* **175**, 112772 (2019).
- <sup>38</sup>J. Y. Byeon, F. T. Limpoco, and R. C. Bailey, "Efficient bioconjugation of protein capture agents to biosensor surfaces using aniline-catalyzed hydrazone ligation," *Langmuir* **26**, 15430–15435 (2010).
- <sup>39</sup>F. Zeighami and M. A. Tehran, "Developing optically efficient nanofiber coatings inspired by *Cyphochilus* white beetle," *Journal of Industrial Textiles* **46**, 495–509 (2016).